Optical transmission spectroscopy of switchable yttrium hydride films

M. Kremers, N. J. Koeman, and R. Griessen
Institute COMPAS, Faculty of Physics and Astronomy, Vrije Universiteit, 1081 HV Amsterdam, The Netherlands

P. H. L. Notten, R. Tolboom, P. J. Kelly, and P. A. Duine
Philips Research Laboratories, Prof. Holstlaan 4, 5656 AA Eindhoven, The Netherlands

(Received 29 July 1997)

The optical transmission of the recently discovered switchable yttrium hydride films is determined spectroscopically as a function of hydrogen content. This is done during electrochemical loading of Pd-capped Y film electrodes, thereby continuously changing the hydrogen concentration. The effect of the Pd cap layer on the film transmission is determined from measurements on a series of films with varying Pd layer thickness. The results are in good agreement with transmission measurements of *in situ* gas phase loaded, uncapped Y films. Both data sets can be consistently described with simple optical decay lengths such as 277.8 nm for $YH_{3-\delta}$ and 15.1 nm for Pd at $\hbar\omega = 1.96$ eV. The hydrogen concentration dependence of the optical transmission is discussed and compared with previous optical measurements on bulk samples and band-structure calculations. [S0163-1829(98)05004-8]

I. INTRODUCTION

A metal insulator (MI) transition with spectacular optical changes in the visible part of the spectrum was reported by Huiberts *et al.*[1] in hydride-forming yttrium and lanthanum films. These films are covered with a thin Pd layer to enhance the hydrogen uptake kinetics and to protect the yttrium or lanthanum layer against oxidation. The MI transition is special in the sense that it occurs at room temperature, is reversible, relatively fast and is the result of a variation in hydrogen concentration. Thus at room temperature one can study the transition in great detail just by varying the hydrogen gas pressure (between typically 1 bar and 10^{-3} mbar), and visually observe the drastic changes in optical properties. This phenomenon is not unique to yttrium and lanthanum, but occurs furthermore in the wide class of trihydride forming rare-earth metals and even in alloys.[2,3]. Recently, it was shown that reversible optical switching can also be accomplished electrochemically using hydride-forming films as electrodes.[4]

The electronic nature of the optically transparent state in yttrium and lanthanum hydrides is presently not well understood, and has, therefore, stimulated the interest of theoreticians.[5,6] Kelly, Dekker, and Stumpf[5] used local-density-approximation (LDA) calculations to search for a minimal total-energy configuration of the hydrogen atoms in hexagonal YH_3 using a Car-Parinello code. They obtained a modified HoD_3 (Ref. 9) configuration, in which subtle displacements of (mainly) H atoms break the inversion and glide plane symmetry, thereby opening a gap in the (single particle) density of states. Ng *et al.*,[6] on the other hand, suggested that strong electron correlation effects, that are not treated in LDA calculations, are important in reducing the width of the H^- bands, by causing electrons to be highly localized on the H atom sites. This strong localization of two electrons in a sort of Zhang-Rice singlet leads to a natural explanation of the fact that not only YH_3 but even still $YH_{2.9}$ is a transparent semiconductor. Very recently, Eder, Pen, and Sawatzky[7] discussed the possibility of a Kondo-lattice effect resulting from the strong hydrogen $1s$-orbital radius on the occupation number. In particular, they show that this extremely strong dependence of the effective hydrogen radius (approximately 0.6 Å for neutral H and 1.6 Å for the negative H^- ion) leads to the formation of bound states similar to the Zhang-Rice singlet in superconducting cuprates.[8]

In this paper the optical transmission of yttrium hydrides is investigated spectroscopically with electrochemical control of the hydrogen concentration. The advantage over gas-phase loading is that this concentration can be varied with a chosen, constant rate. We show that it is possible to correct for the effect of Pd and to determine the intrinsic optical transmission of YH_x for $0 \leqslant x < 3$ in the photon energy range $1.1\ \text{eV} \leqslant \hbar\omega \leqslant 2.0\ \text{eV}$. To our knowledge, this is the first time that spectroscopic data are presented as a function of continuously varied hydrogen concentration in one and the same YH_x sample. These electrochemical results are compared with combined measurements of both optical transmission at $\lambda = 632.8$ nm (i.e., $\hbar\omega = 1.96$ eV) and electrical resistivity on as-deposited, uncapped yttrium films during *in situ* hydrogen absorption. The measured optical transmission is mapped onto hydrogen concentrations by using the results of the electrochemical loading experiments. In this way the intrinsic hydrogen concentration dependence of the resistivity is also determined for uncapped yttrium hydride films.

II. EXPERIMENT

By increasing, at room temperature, the hydrogen concentration x in YH_x from 0 to 3, three stable hydride phases are encountered, denoted α^*, β, and γ.[10,11] In addition, there are two regions of coexisting phases ($\alpha^* + \beta$ and $\beta + \gamma$). A section of the phase diagram at room temperature is shown in Fig. 1. In order to change the hydrogen concentration, two methods have been used: (i) electrochemical (de)hydrogenation and (ii) *in situ* gas (de)hydrogenation.

For the electrochemical experiments, yttrium films of

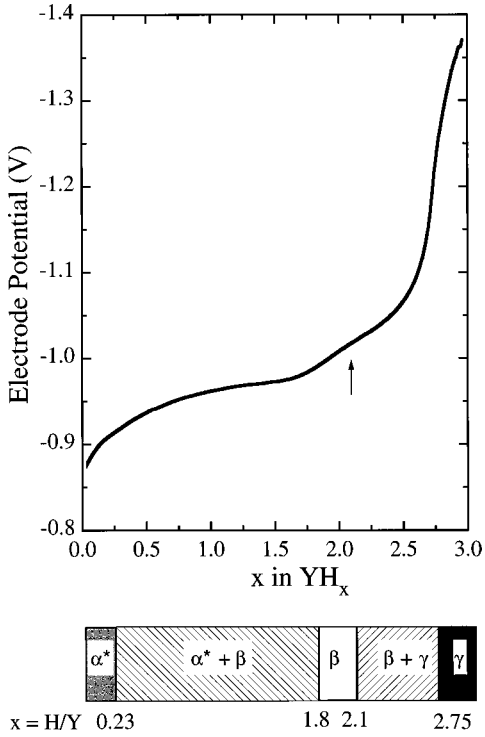

FIG. 1. Development of the electrode potential as a function of the calculated hydrogen concentration for a 500-nm Y film electrode covered with a 5-nm Pd cap layer during galvanostatic hydrogenation with a current of $I=-1$ mA in 6-M KOH. The arrow points out the existence of a subtle feature at $x\approx 2.1$. Also denoted are the room-temperature phases α^*, β, and γ, and the regions with coexisting phases $\alpha^*+\beta$ and $\beta+\gamma$, according to Refs. 10 and 11.

500-nm thickness were evaporated by means of an electron gun in a UHV system (background pressure 10^{-8} mbar) on quartz (SiO_2) substrates. They were subsequently capped *in situ* with thermally evaporated Pd layers of 5-, 9-, 14-, and 20-nm average thickness, respectively. These films have been used as working electrodes during so-called galvanostatic (i.e. constant current) loading experiments in a three-electrode setup using an open cuvet with flat, parallel windows (for details see Ref. 4). The electrolyte was 6-M KOH to prevent dissolution of the extremely base Y. The counter electrode was Pt and the reference electrode was Hg/HgO. All potentials are given with respect to this reference. The electrochemical cell was placed in the light path of a Fourier transform infrared spectrometer (Bruker IFS 66), so that during loading optical transmission spectra could be recorded in typically a few seconds, which is small compared to the total duration ($\approx$30 min) of a typical galvanostatic experiment. The light used was limited to the photon energy range $1.1\ \text{eV}\leqslant\hbar\omega\leqslant 2$ eV in order to avoid photoanodic dissolution of semiconducting $YH_{3-\delta}$ [band gap ≈ 2 eV (Ref. 2)]. The lower limit of 1.1 eV is due to the Si-diode detector used. This photon energy range allows to study the typical optical behavior near the MI transition, as well as near the yttrium dihydride composition.

The change in hydrogen concentration, Δx, during an experiment is calculated from the Y film thickness d, the electrode surface area A (here typically 2.6 cm^2), the molar volume of yttrium, V, and the integrated charge flow through the electrode:

$$\Delta x=-\frac{V}{Ad}\frac{\int I dt}{F}, \tag{2.1}$$

where I is the current and F is Faraday's constant. The errors in A and d can be kept within 3%.[4] Films that have not been hydrided before may still contain some hydrogen due to incorporation during evaporation or storage. Equation (2.1) may overestimate the concentration if (i) hydrogen is consumed for the reduction of oxygen dissolved in the electrolyte,[4] (ii) H_2 gas is formed, or (iii) a portion of uncapped Y is oxidized and can therefore not be hydrided. Although Pd also forms a hydride, the amount of hydrogen absorbed in the Pd cap layer can be neglected, because it is relatively thin and the enthalpy of formation of PdH_x is much less negative than that of YH_x. It will be shown that the total error in hydrogen concentration is in fact not larger than 0.1 near $x=3$.

For the *in situ* hydrogen gas loading experiments, yttrium films were evaporated on sapphire (Al_2O_3) substrates in another UHV system (background pressure 10^{-9} mbar). The film thickness was typically 200–500 nm. Note that no capping whatsoever was used. Such a sample was transported under UHV conditions to a hydrogen loading chamber which was attached to the UHV evaporation chamber. The sample was first subjected to very clean hydrogen produced by heating a previously hydrided Ti spiral. Subsequently, hydrogen gas was admitted from a 5-N H_2 bottle via outgassed pipes and a leak valve until a final H_2 pressure of 1 bar was reached. During this process the four-point resistivity was measured using gold-coated resistance probes pressed onto the film with a spring force of 0.5 N. These could be manipulated from outside the UHV chamber. Moreover, the sample was positioned between two glass prisms mounted inside the loading chamber. It was therefore possible to direct a laser beam (i.e., a HeNe laser with $\lambda=632.8$ nm) from outside the chamber through subsequently: a UHV window, the first prism, the yttrium film, the second prism and finally through a second UHV window into a photodiode detector. In this way, optical transmission and resistivity measurements could be performed simultaneously.

III. RESULTS OF GALVANOSTATIC LOADING

In Fig. 1, the measured electrode potential during galvanostatic loading of a virgin Y film (500 nm thick, capped with 5-nm Pd) is plotted. Immediately after applying a $I=-1$ mA loading current, the potential drops to about -0.9 V. In the region $0.23<x<1.75$ the electrode potential only decreases slightly with x. At $x\approx 1.75$, however, there is a clear increase of the slope of the curve. Close observation reveals another, much more subtle, deviation at $x\approx 2.1$. For $x>2.7$, the potential clearly aims at more negative values. Figure 1 also shows the concentration regions corresponding to the room temperature α^* (hcp), β (fcc), and γ (hcp), and the mixed phases as known for bulk YH_x.[10,11] As explained in a previous paper,[4] the measured electrode potential indicates that the so-called β-γ plateau[2] in the pressure-composition isotherm of YH_x can be found in the region $2.1<x<2.7$. The potential finally reaches a constant value at which hydrogen gas evolution takes place, and the calculation of Δx according to Eq. (2.1) becomes inaccurate. In all

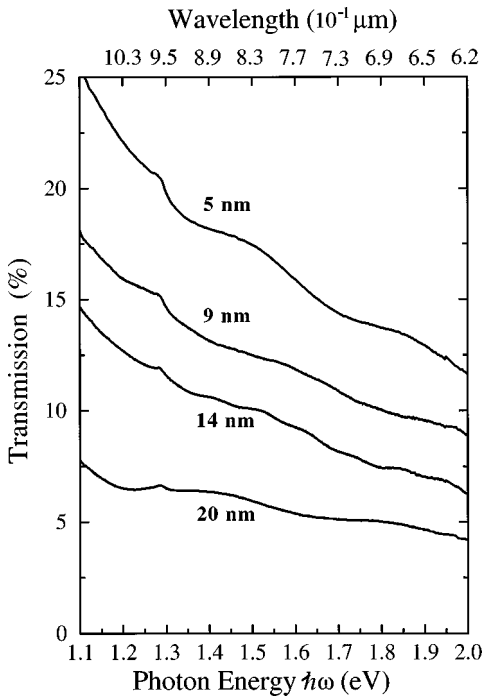

FIG. 2. Transmission spectra of four 500-nm-thick $YH_{3-\delta}$ films, capped with 5-, 9-, 14-, and 20-nm Pd, respectively, at the highest final concentrations reached.

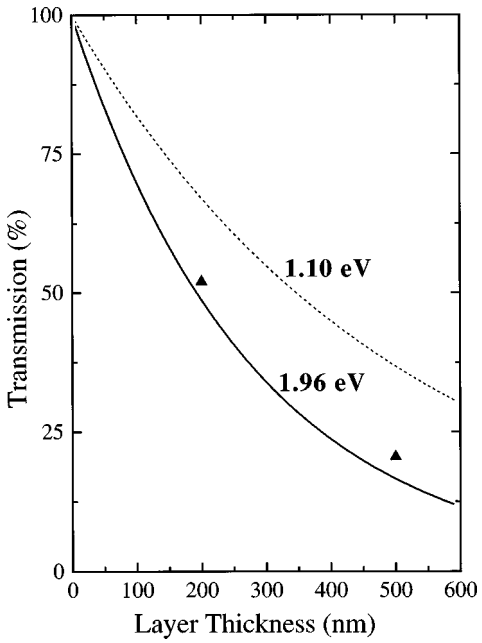

FIG. 3. Predicted layer thickness dependencies of the optical transmission of uncapped $YH_{x\approx 3}$ films using the optical decay length $\lambda_{YH_{3-\delta}} = 277.8$ nm at $\hbar\omega = 1.96$ eV (full curve) and $\lambda_{YH_{3-\delta}} = 500$ nm at $\hbar\omega = 1.1$ eV (dashed curve) determined from the measurements in Fig. 2. The triangular points represent measurements of the optical transmission ($\hbar\omega = 1.96$ eV) of two actually uncapped films (500 and 200 nm) as determined by *in situ* loading in 1-bar H_2 gas.

experiments the current was turned off exactly at this point. As can be seen from Fig. 1, the hydrogen concentration x is then close to 3. The final compositions $YH_{3-\delta}$ reached in this way for the four electrodes considered in this work can be assumed to be nearly equal, as, past the β-γ plateau; only very large differences in chemical potential can cause appreciable concentration differences.[2] The transmission spectra of the four films at this final composition are plotted in Fig. 2.

Using macroscopic thin film optics, the contribution of Pd is estimated by fitting the data in Fig. 2 to the following equation:

$$T_{YH_{3-\delta}/Pd}(\hbar\omega) = e^{-\lambda_{Pd}^{-1}(\omega)d_{Pd}} e^{-\lambda_{YH_{3-\delta}}^{-1}(\omega)d_{YH_{3-\delta}}}, \quad (3.1)$$

where T is the transmisson, d_i the layer thickness and λ_i the characteristic optical decay length ($i =$ Pd or $YH_{3-\delta}$). This procedure gives a convincingly consistent behavior for both λ_{Pd} and $\lambda_{YH_{3-\delta}}$ over the total photon energy range studied. At $\hbar\omega = 1.96$ eV, for example, the following values are obtained: $\lambda_{YH_{3-\delta}} = 277.8$ nm and $\lambda_{Pd} = 15.1$ nm. The transmission of uncapped $YH_{3-\delta}$ layers can, accordingly, be estimated by

$$T_{YH_{3-\delta}}(\hbar\omega) = e^{-\lambda_{YH_{3-\delta}}^{-1}(\omega)d_{YH_{3-\delta}}}. \quad (3.2)$$

Figure 3 shows the layer thickness dependence of the optical transmission at $\hbar\omega = 1.96$ and 1.1 eV predicted by Eq. (3.2). The two filled triangles added to the figure represent measurements at $\hbar\omega = 1.96$ eV of actually uncapped films of respectively 500 and 200 nm obtained by *in situ* gas-phase loading. There is good agreement between these *in situ* measurements and the predictions from the electrochemical results represented by the full line. Therefore, all transmission data presented further on have been corrected for the effect of the Pd cap layer by means of the procedure described above.

Figure 4 is a three-dimensional representation of the optical transmission spectra measured as a function of hydrogen concentration during the first galvanostatic loading ($I = -1$ mA) of the 5-nm Pd capped 500-nm Y film. For concentrations up to $x \approx 1.7$ there is no detectable transmission.

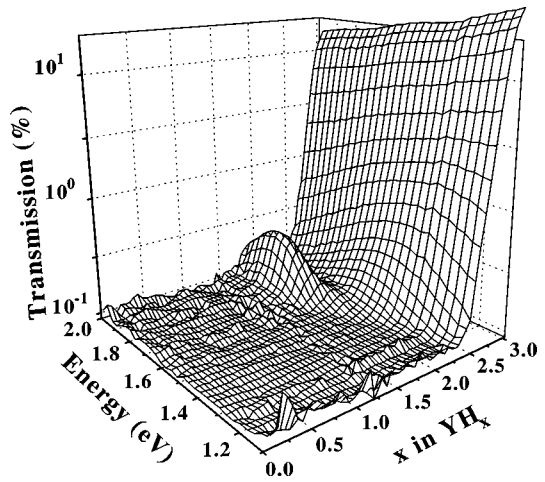

FIG. 4. Three-dimensional representation of the optical transmission as a function of photon energy and calculated hydrogen concentration for a 500-nm Y film electrode covered with a 5-nm Pd top layer during galvanostatic hydriding (−1 mA) in 6-M KOH. Note that the data, which are obtained during the same experiment as in Fig. 1, are corrected for the effect of Pd.

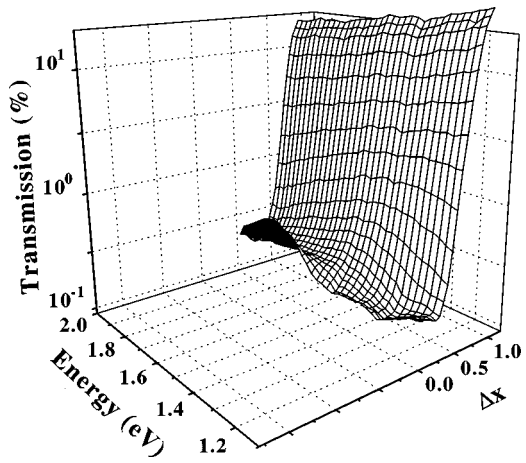

FIG. 5. Optical transmission as a function of photon energy and calculated hydrogen concentration change $\Delta x = \Delta(H/Y)$ for a 500-nm Y film electrode covered with a 5-nm Pd cap layer during the second galvanostatic hydriding (-1 mA) in 6-M KOH. The data are corrected for the effect of Pd, and plotted so as to allow for an easy comparison with the results of the first hydrogen loading in Fig. 4.

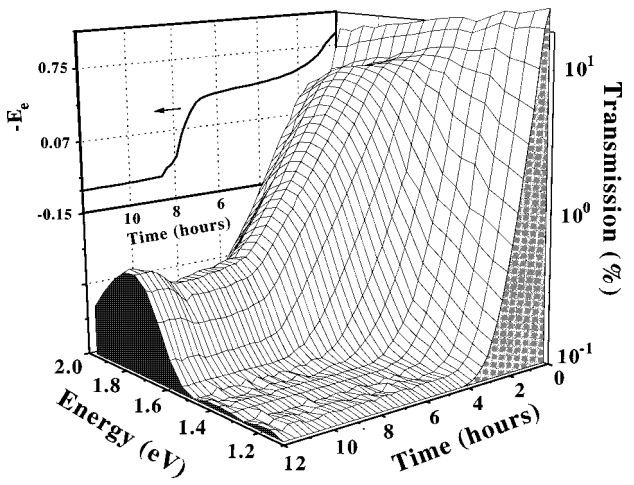

FIG. 6. Optical transmission as a function of photon energy and time for a 500-nm Y film electrode covered with a 5-nm Pd top layer during open circuit relaxation immediately after the second galvanostatic charging represented in Fig. 5. The data are corrected for the effect of Pd. The time is plotted in this unconventional manner to allow for an easy comparison with the hydrogen absorption data in Fig. 4. The inset shows the development of the simultaneously measured electrode potential E_e that is a measure for the chemical potential of hydrogen at the surface of the electrode.

A little transmission hill (note the logarithmic scale) is visible for $1.7 \leqslant x \leqslant 2.1$ and $1.6 \leqslant \hbar\omega \leqslant 2$ eV (i.e., in the red part of the visible spectrum). This hydrogen concentration interval corresponds well to the stability region of the β-yttrium-dihydride phase. When the concentration is raised above 2.1, the transmission continues to decrease up to $x \approx 2.3$. As the tetrahedral interstitial sites are filled during the formation of yttrium dihydride, hydrogen here occupies the octahedral interstitial sites. The optical spectrum at $x = 2.3$ is maximal at $\hbar\omega = 1.5$ eV, i.e., the transmission is smaller for both higher and lower energies. Upon increasing the concentration to $x = 2.7$ the maximum gradually becomes larger and shifts to lower energies, i.e. to $\hbar\omega = 1.2$ eV at $x = 2.7$. For each concentration $x > 2.7$ such a maximum is no longer observed. The transmission is then everywhere a continuously decreasing function of photon energy (in the region under consideration).[12]

In order to study the reproducibility of the MI transition, the electrode was first discharged to the β-dihydride phase. It is not possible to decrease the concentration further, because the corresponding partial hydrogen gas pressures then become too small to be realized (e.g., 10^{-28} Pa on the α^*-β plateau[4]). Consequently the second charging must start from a concentration $1.8 \leqslant x \leqslant 1.9$ within the β phase. The final concentration is limited to $x = 3$. Therefore, a total concentration change $1.1 \leqslant \Delta x \leqslant 1.2$ is expected. Figure 5 shows the measured optical transmission as a function of Δx, and the highest value reached is $\Delta x = 1.2$. The total error in hydrogen concentration must therefore be smaller than 0.1. The reproducibility of the MI transition is evident from a comparison with Fig. 4. Immediately after this second charging, the current is interrupted, and the development of the optical transmission, shown in Fig. 6, is followed under open-circuit conditions. The hydrogen absorbed by the electrode is then consumed for the reduction of oxygen dissolved in the electrolyte. As the corresponding (average) oxygen reduction current density is only of the order of 6×10^{-6} A/cm^2, a very small hydrogen desorption rate is found. This can be exploited to study the electrode potential under quasiequilibrium conditions. This potential E_e is plotted in the inset of Fig. 6. Assuming the oxygen reduction rate to be more or less constant in time, one can interpret the time axis of Fig. 6 as concentration axis. The MI transition sets in almost immediately at relatively high concentrations, before E_e reaches an almost constant value that is prolonged for about 5 h. Via the chemical potential of hydrogen[4] E_e translates into a hydrogen gas pressure P_{H_2}, according to

$$E_e = -0.926 - \frac{RT}{2F} \ln P_{H_2}, \tag{3.3}$$

where T is the temperature and R is the gas constant. The constant value of E_e therefore corresponds to the β-γ plateau. During desorption one therefore concludes that the MI transition takes place in the γ phase. In Fig. 6 an additional temporary transmission stabilization is observed in the region $1.7 \text{ eV} \leqslant \hbar\omega \leqslant 2$ eV. This structure is absent during galvanostatic loading. Results of experiments that clarify the origin of this structure will be published in the near future.[13] The subsequent transmission suppression that occurs before the typical dihydride transmission spectrum is obtained is less pronounced than found during charging. Despite these differences, Figs. 4 and 6 exhibit the same general behavior.

IV. RESULTS OF *IN SITU* LOADING

In Sec. III the optical transmission was determined as a function of hydrogen concentration, and it was shown that one can correct for the effect of the Pd layer. It is, however, not easy to measure reliably the electrical resistivity of electrodes during electrochemical experiments (see Refs. 14 and 15). *Ex situ* resistivity measurements during gas-phase loading, as performed by Huiberts and co-workers[1,16] on Pd-

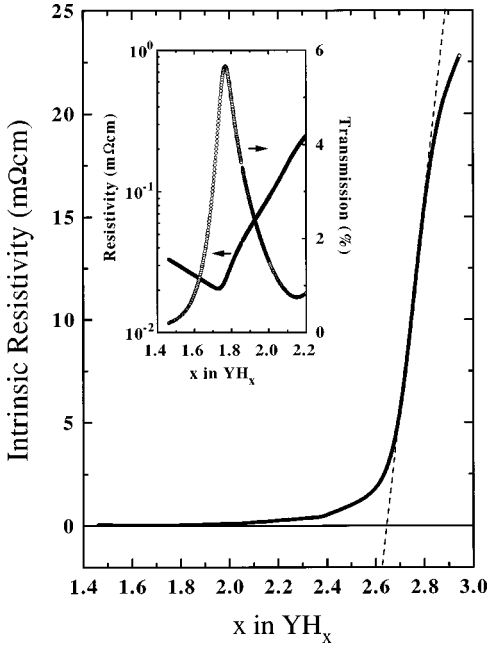

FIG. 7. Hydrogen concentration dependence of the electrical resistivity of an *in situ* loaded 200-nm yttrium film without Pd capping. This curve has been obtained from a mapping of the optical transmission at $\hbar\omega = 1.96$ eV (simultaneously measured with this resistivity) onto the transmission as a function of the electrochemically measured hydrogen concentration. The inset shows the behavior of both the transmission and electrical resistivity near the yttrium-dihydride composition.

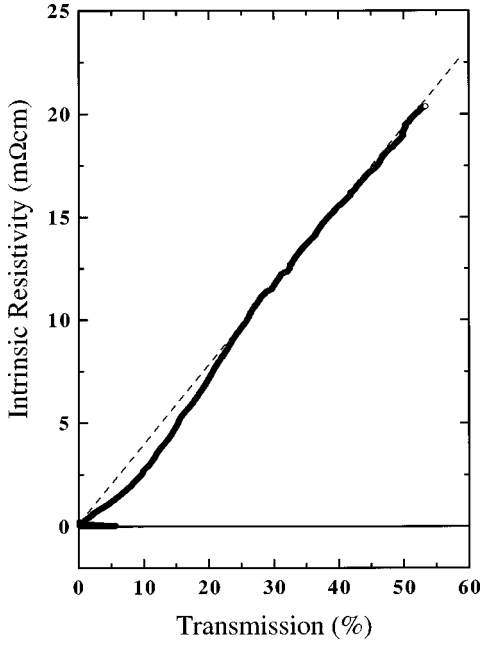

FIG. 8. Optical transmission at $\lambda = 632.8$ nm vs electrical resistivity for the same *in situ* loading experiment as in Fig. 7 involving a 200-nm uncapped yttrium film. Note the surprising linear relation between both quantities for resistivities larger than 9 mΩ cm.

capped films, always suffer from the partial short circuiting by the Pd and the fact that the hydrogen concentration is not determined. It is, however, possible to load uncapped yttrium films with hydrogen, as demonstrated by Curzon and Singh.[17,18] These authors measured the resistivity of relatively thin yttrium layers. In the present work the resistivity of uncapped, relatively thick, yttrium-hydride films is presented. Yttrium layers of both 200- and 500-nm thicknesses were loaded up to the trihydride state, clearly showing the MI transition in the simultaneously measured resistivity and optical transmission (at $\hbar\omega = 1.96$ eV). The hydrogen uptake rate was found to be strongly dependent on the purity of the hydrogen gas. The catalytic activity of yttrium itself for hydrogen dissociation must therefore be appreciable, but very sensitive to poisoning of the surface (probably caused by oxidation).

The resistivity of the unhydrided 200-nm yttrium film was 95 $\mu\Omega$ cm. This is closer to the bulk value of 63 $\mu\Omega$ cm than the 125 $\mu\Omega$ cm obtained by Curzon and Singh[18] for a similar film. By comparing the time dependence of the measured transmission with the electrochemically measured concentration dependence of the optical transmission it was possible to derive the time dependence of the concentration in the *in situ* experiment. The result of this procedure is used to plot the intrinsic resistivity versus the calculated hydrogen concentration for the YH_x film of 200 nm in Fig. 7. In the region $2.7 \leqslant x \leqslant 2.8$ the resistivity increases fastest and almost linearly with concentration. The inset of Fig. 7 shows the behavior of both transmission and resistivity near the yttrium dihydride composition. The transmission maximum almost coincides with the well-known minimum in resistivity for yttrium dihydride.

In Fig. 8 the resistivity is plotted against the simultaneously measured transmission. An unexpected linear dependence of resistivity on transmission is clearly present where the resistivity is larger than 9 mΩ cm. This is indicated by the dashed line that even crosses the point where the resistivity and transmission would simultaneously be zero. From Fig. 7 one can see that $\rho > 9$ mΩ cm corresponds to $x > 2.73$. The linear dependence between intrinsic resistivity and transmission (at $\hbar\omega = 1.96$ eV) is therefore found to be property of the γ-yttrium-trihydride phase. In the β-γ coexistence region the resistivity can be considered to be lagging somewhat behind the transmission.

V. DISCUSSION

The most important result of this paper is represented by Fig. 4. The development of the optical transmission as a function of hydrogen concentration can be discussed in terms of the various regions in the YH_x phase diagram. The optical transmission of a thin film is in principle determined by both the absorption and reflection (and possibly scattering) of light. Up to concentrations far into the α^*-β coexistence region (up to $x \leqslant 1.7$), no light is transmitted as is expected for a metallic film of 500 nm.

For $1.75 \leqslant x \leqslant 2.1$ the film will be predominantly in the stability region of the β-yttrium-dihydride phase. It is clear that there is a maximum in the transmission centered at $\hbar\omega = 1.8$ eV causing a reddish appearance in transmission. The onset can be understood in terms of the gradual increase of the fraction of β phase in the sample in the α^*-β coexistence region. By means of absorptivity measurements on a sample of $YH_{1.73}$, Weaver, Rosei, and Peterson[20] constructed the complex dielectric function for this composition.

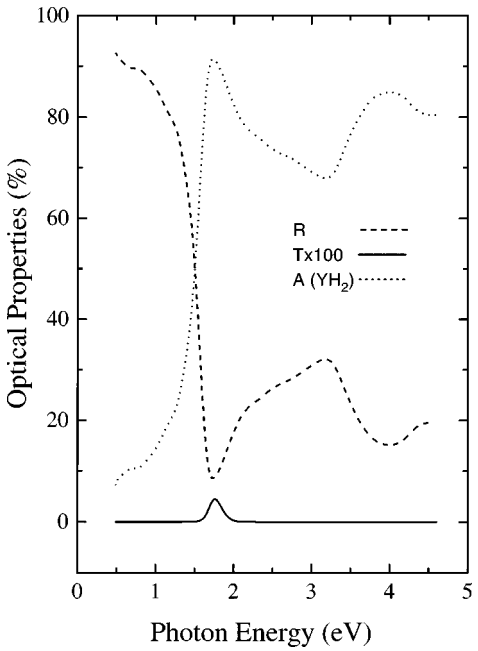

FIG. 9. Calculated optical properties of the multilayer configuration as used in the experiments, consisting of a 20-nm palladium cap layer and a 500-nm layer of yttrium dihydride on top of a transparent substrate when backilluminated from the yttrium-dihydride side. Input data were taken from Refs. 20 and 21.

These measurements could be interpreted in terms of self-consistent band-structure calculations by Peterman *et al.*[19] for stoichiometric YH_2 with all tetrahedral sites filled by hydrogen. The reddish transmission of yttrium dihydride can be understood accordingly. On the low-energy side, $\hbar\omega < 1.5$ eV, there is no transmission, since almost all of the light is reflected by the electrons in the band crossing the Fermi level. This behavior is typical of a Drude-like free-electron plasma (intraband transitions). The corresponding plasmon is screened by the occurrence of interband transitions. Although the density of states is not negligible above the Fermi energy, the onset of interband transitions is calculated to be roughly at 2 eV. The absorption of photons therefore only becomes appreciable for energies $\hbar\omega \geqslant 2$ eV.[20] In the region $1.5 \leqslant \hbar\omega \leqslant 2$ eV there is neither strong reflection nor strong absorption of light, and photons can be transmitted. Using the dielectric function from Ref. 20 and the refractive index for (thin) film Pd from Ref. 21, the optical transmission, absorption and reflection can be calculated for the type of samples as were used here. The result of this calculation is given in Fig. 9. Exactly in the region $1.5 \leqslant \hbar\omega \leqslant 2.0$ eV a (small) peak in the transmission is obtained.

When the concentration is increased above $x=1.9$ the transmission first decreases. A close look at the experimental data shows that the photon energy at which the transmission is maximal shifts to lower energies with increasing x. This behavior is also consistent with the observations of Ref. 20. The authors attributed the decreasing transmission to extra absorption at low energies, caused by the filling of octahedral sites. Furthermore, a shift of the plasma frequency to lower energies was observed and explained in terms of enhanced screening. The shift of both the onset of interband transitions and the plasma frequency explains the shift of the transmission maximum to lower energies as observed in Fig. 4. At the highest concentration in the β-dihydride phase, $x=2.1$, the absorption has become so large that hardly any transmission can be detected in the considered photon energy range.

At $x=2.1$ the β-γ coexistence region is entered. Upon raising the concentration one expects an increasing volume fraction of the film to be converted into hexagonal γ-trihydride with a composition corresponding to the lowest stable concentration of this phase (i.e., $x \approx 2.75$ at room temperature). By means of optical microscopy we have not been able to observe nucleation of this phase. The nuclei may be too small (i.e., $<1\ \mu m^3$) or too weakly transmitting to be observed. Another explanation is that the γ-phase nucleates as a two-dimensional layer at the surface of the film, and that its thickness increases with increasing hydrogen concentration. A simple calculation along the lines of Eq. (3.1) shows that for such a bilayer $\ln T$ is a linear function of x, as is observed. The shape of the transmission spectra of course also holds information about the composition of the film. It is expected that at some concentration the total volume of the film consists of single-phase semiconducting material, and that consequently the optical transmission decreases with photon energy to disappear near the absorption edge. Only the spectra for $x>2.7$ have such a shape.

If the measured transmission is considered on a linear scale instead of a logarithmic scale, though, it is clear that the transmission starts to increase considerably only for $x>2.7$. At $x=2.75$ it is believed that the film consists of purely γ phase and it is here where the transmission increase with concentration is especially steep, also in the logarithmic plot. This might suggest that the MI transition is related to the fcc(β)-hcp(γ) phase transition. It is possible, however, to sputter deposit yttrium films that do not show a fcc-hcp structural phase transition (they remain cubic),[22] but that do exhibit the MI transition. Moreover, they are transparent when x approaches 3. In addition, it is known that lanthanum hydride, LaH_x, also shows switchable optical properties and this material is cubic for all $x \geqslant 2$. Both cases exemplify that the MI transition is not driven by a structural phase transition.

It is important to note that for all concentrations $x>2.7$ the measured transmission is a monotonically decreasing function of photon energy. This behavior is typical for a system with a gap in the excitation spectrum (i.e., an absorption edge). Nevertheless, the transmission continues to increase with x in this region. Gas-phase loading experiments also show that the transmission is not yet saturated at pressures of 1-bar H_2. This implies that the intrinsic transmission of stoichiometric YH_3 can be higher than predicted in Fig. 3. It furthermore suggests that octahedral hydrogen vacancies dominate the optical properties of $YH_{3-\delta}$. Ng *et al.*[6] put this fact forward as evidence of the importance of strong electron correlation effects. From the above-presented experiments, it is clear that in a concentration interval of the order of 0.3 H per Y (from $YH_{2.7}$ to YH_3), an optical behavior is found that is consistent with a gap in the electronic excitation spectrum. If stoichiometric YH_3 is a clean semiconductor, one expects that a hydrogen vacancy level of the order 0.3 introduces far too much doping for the observed behavior, unless there is

indeed considerable carrier localization, due to, for example, disorder or electron correlation effects. In the model of Ng *et al*. vacancies do indeed act as very localized donors.

VI. CONCLUSIONS

The optical properties of YH_x electrodes have been determined continuously as a function of x in a single sample during galvanostatic (de)hydriding. The measured optical transmission spectra, corrected for the contribution of the Pd cap layer, compare well with results obtained for *in situ* gas-phase loaded uncapped yttrium films. For 500-nm films the maximum transmission of yttrium dihydride is typically 0.25% ($\hbar\omega = 1.8$ eV). At the same energy the maximum transmission of the substoichiometric trihydride is typically 16%.

The behavior of the optical transmission near the dihydride composition can be qualitatively understood in terms of interband and intraband transitions. Both the maximum of this reddish transmission window and the minimum in electrical resistivity can be taken as a characteristic of the β phase, as they occur simultaneously.

For $x \geqslant 2.7$ the optical transmission behavior confirms the presence of a semiconducting gap, but continues to increase with x. A clear interpretation of this behavior is not yet available. More experimental and theoretical work is evidently needed to reveal the precise nature of the switching transition in yttrium hydride.

ACKNOWLEDGMENTS

We thank J. N. Huiberts at the Vrije Universiteit, and M. Ouwerkerk, P. van der Sluis, and F. J. A. den Broeder at Philips Research Laboratories for very interesting and stimulating discussions. In addition we would like to thank F. C. Zhang, T. M. Rice, R. Eder, and G. Sawatzky for illuminating discussions about the electronic structure of switchable hydrides.

[1] J. N. Huiberts, R. Griessen, J. H. Rector, R. J. Wijngaarden, J. P. Dekker, D. G. de Groot, and N. J. Koeman, Nature (London) **380**, 231 (1996).

[2] R. Griessen, J. N. Huiberts, M. Kremers, A. T. M. van Gogh, N. J. Koeman, J. P. Dekker, and P. H. L. Notten, J. Alloys Compd. **44**, 253 (1997).

[3] P. van der Sluis, M. Ouwerkerk, and P. A. Duine, Appl. Phys. Lett. **70**, 3356 (1997).

[4] P. H. L. Notten, M. Kremers, and R. Griessen, J. Electrochem. Soc. **143**, 3348 (1996).

[5] P. J. Kelly, J. P. Dekker, and R. Stumpf, Phys. Rev. Lett. **78**, 1315 (1997).

[6] K. K. Ng, F. C. Zhang, V. I. Anisimov, and T. M. Rice, Phys. Rev. Lett. **78**, 1311 (1997).

[7] R. Eder, H. F. Pen, and G. Sawatzky, Phys. Rev. B **56**, 10 115 (1997).

[8] R. Griessen, Phys. Blätter **12**, 1207 (1997).

[9] T. J. Udovic, Q. Huang, and J. J. Rush, J. Phys. Chem. Solids **57**, 423 (1996).

[10] P. Vajda, in *Handbook on the Physics and Chemistry of Rare Earths*, edited by K. A. Schneidner Jr. and L. Eyring (Elsevier, Amsterdam, 1995).

[11] W. M. Mueller, J. P. Blackledge, and G. G. Libowitz, *Metal Hydrides* (Academic, New York, 1968).

[12] J. N. Huiberts, J. H. Rector, R. J. Wijngaarden, S. Jetten, D. de Groot, B. Dam, N. J. Koeman, Y. S. Cho, B. Hjörvarsson, S. Olafsson, and R. Griessen, J. Alloys Compd. **239**, 158 (1996).

[13] M. Kremers, P. H. L. Notten, M. Ouwerkerk, and R. Griessen (unpublished).

[14] R. I. Tucceri and D. Posadas, J. Electrochem. Soc. **128**, 1478 (1981).

[15] T. Dickinson and P. R. Sutton, Electrochim. Acta **19**, 427 (1974).

[16] J. N. Huiberts, R. Griessen, C. van Haesendonck, R. J. Wijngaarden, and M. Kremers, Phys. Rev. Lett. **79**, 3724 (1997).

[17] A. E. Curzon and O. Singh, J. Phys. F **8**, 1619 (1978).

[18] A. E. Curzon and O. Singh, Thin Solid Films **57**, 157 (1979).

[19] D. J. Peterman, B. N. Harmon, J. Marchiando, and J. H. Weaver, Phys. Rev. B **19**, 4867 (1979).

[20] J. H. Weaver, R. Rosei, and D. T. Peterson, Phys. Rev. B **19**, 4855 (1979).

[21] A. Borghesi and A. Piaggi, in *Handbook of Optical Constants of Solids II*, edited by E.D. Padik (Academic, New York, 1991).

[22] M. Ouwerkerk and F. J. A. den Broeder (private communications).